Polyelectrolyte uptake by PEMs: Impacts of molecular weight and counterion

Xingjie Zan [a], David A. Hoagland [b], Tian Wang [a], Bo Peng [a], Zhaohui Su [a],*

[a] State Key Laboratory of Polymer Physics and Chemistry, Changchun Institute of Applied Chemistry, Chinese Academy of Sciences, 5625 Renmin Street, Changchun 130022, PR China
[b] Polymer Science and Engineering Department, University of Massachusetts, Amherst, MA 01003, USA

ARTICLE INFO

ABSTRACT

Presented with an elevated level of aqueous salt, a polyelectrolyte multilayer (PEM) swells and subsequently can undergo large mass uptake when exposed to a salt solution containing the capping polyelectrolyte. Features of the uptake depend on the properties of polyelectrolyte (molecular weight, polydispersity, concentration), solvent (salt concentration and ion identities), and PEM (number of layers, polyelectrolyte identities). Here, poly(diallyldimethylammonium chloride)/poly(styrene sulfonate) (PSS) PEMs capped with PSS are investigated by Quartz Crystal Microbalance with Dissipation during successive challenges by salt and PSS. Only when the salt level is substantially higher than at PEM construction, leading to large PEM swelling, does PSS uptake become significant. Steady state uptake grows and then levels off with PSS molecular weight; the crossover to molecular weight independence falls with salt concentration. Across the dilute PSS range, uptake mechanisms are not affected by solution concentration, although at very dilute concentration, the rate limiting process becomes diffusion in solution rather than in PEM. Swelling of PEM by salt, and hence rate of uptake and ultimate uptake, correlate with the salt anion's position in the Hofmeister series.

© 2012 Elsevier Ltd. All rights reserved.

1. Introduction

The uptake of polyelectrolytes by permeable substrates such as porous glasses [1], crosslinked networks [2,3], and fibers [4—6] is central to a range of technologies, including chromatography, paper fabrication, and controlled release [1,7,8]. Substrate permeability distinguishes polyelectrolyte uptake from polyelectrolyte adsorption, but locally, the interactions controlling the two phenomena are similar. In both cases, the capture of polyelectrolyte by charged substrate corresponds to a cooperative ion exchange reaction that forms salt bonds between polyelectrolyte and substrate as small counterions are released. While the release affords a major thermodynamic impetus, uptake nonetheless reflects a delicate balance of electrostatic (and possibly other) actions, some favorable and some disfavorable [9]. For example, the increase of polyelectrolyte charge density promotes attraction to substrate, favoring uptake, but the increase also causes polyelectrolyte stiffening, disfavoring uptake. Such trade-offs, and difficulty in distinguishing between thermodynamic and kinetic control, makes outcomes difficult to predict. Consequently many experiments and theories have been developed to explain the influence of ionic strength, molecular weight, and charge density. Self-consistent mean-field theories [9,10], for example, predict that uptake decreases with ionic strength due to the reduced polyelectrolyte-surface electrostatic attraction under enhanced electrostatic screening. The same theories indicate that surface overcharging emerges in the "screening enhanced regime" if a non-electrostatic interaction between polyelectrolyte and surface is present [11]. It has also been proposed that overcharging occurs due to lateral correlations between attached polyelectrolytes [11—13]. The ratio of pore size to polyelectrolyte coil size is another crucial factor, affected not just by the polyelectrolyte's molecular weight but also by its charge density and concentration.

Several interactions are possible when a polyelectrolyte multilayer (PEM) constructed by the layer-by-layer (LbL) deposition method is challenged with a concentrated salt solution containing similarly charged polyelectrolyte. In one, attractive (non-electrostatic) interactions between polyelectrolyte and PEM cause an initial PEM capture of the polyelectrolyte, the captured polyelectrolyte subsequently diffusing through the PEM's outer layers to find the first available region of opposite charge, there becoming fixed [4—6]. In another, starting with the same attachment step, polyelectrolytes distribute across the PEM through a "relay race" mechanism in which the polyelectrolytes displace inward by a cascade of inter-polyelectrolyte exchange reactions [3]. Polyelectrolyte uptake by like-charged soluble polyelectrolyte

* Corresponding author. Tel.: +86 431 85262854; fax: +86 431 85262126.
E-mail addresses: xjzan2000@hotmail.com (X. Zan), hoagland@mail.pse.umass.edu (D.A. Hoagland), wangtian@ciac.jl.cn (T. Wang), pengbo@ciac.jl.cn (B. Peng), zhsu@ciac.jl.cn (Z. Su).

complexes (PECs) has been studied extensively by experiment [14–16] and theory [17–19], with considerable attention directed at bio-polyelectrolytes and their PECs, which have potential applications in protein purification, drug delivery, and food technology [19,20]. Uptake, again primarily directed by electrostatics, redistributes polyelectrolytes and counterions among solution and PECs [21]. LbL construction of PEMs mandates charge overcompensation after each deposition, with chains of the capping polyelectrolyte to some extent penetrating previous layers [22,23]. During construction at high salt, the penetration is enhanced [24]. Although many publications describe factors controlling PEM growth [25,26], few explain mechanistically how these factors affect polyelectrolyte uptake and diffusion, probably because technologies for monitoring such ultra-thin films are scarce.

The Quartz Crystal Microbalance with Dissipation (QCM-D) method, based on an acoustomechanic transducer principle, offers characterization of surface-confined films *in situ* and in real time. By measuring shifts in resonant frequency (Δf) and energy dissipation (ΔD) of an oscillating sensor crystal, the absorbed mass of a thin film is obtained alongside information about the film's mechanical properties, dynamics, and hydration [27]. In a previous report, we showed that QCM-D conveniently reports the uptake of poly(styrene sulfonate) (PSS) by poly(diallyldimethyl ammonium chloride) (PDDA)/PSS PEMs capped with PSS [28]. This report found that PSS uptake could be dramatically enhanced by prior exposure of the PEMs to a salt concentration well above that of PEM construction; such exposure swells the film, loosening polyelectrolyte–polyelectrolyte contacts and thereby enabling augmented PSS uptake. The ultimate uptake level rises sharply with the salt concentration, and at least for high salt concentrations, the uptake appears controlled by diffusion in the PEM. When steady state is achieved, the added PSS at such salt concentrations appears to permeate the film.

In the present work, using the same approach and starting PEMs, PSS uptake is tracked as parameters characterizing the PSS 'challenger' are varied, including its molecular weight (M), concentration, and counterion. The aim is to elucidate how these factors influence uptake, and from this knowledge, to expand PEM growth and modification strategies.

2. Experimental section

2.1. Materials

A PSS sample of moderate molecular weight M ($\sim$70,000 g/mol) and broad polydispersity ($\sim$2.7), designated PSS-0, and a PDDA sample of moderate M (20 wt % in water, $M \sim$ 200,000–350,000 g/mol) were both purchased from Aldrich; the materials were used as received. Additional PSS samples of narrower polydispersity were obtained from Scientific Polymer Products, Inc. and designated PSS-1, PSS-2, PSS-3, and PSS-4; their respective molecular weight and polydispersity were 16,000 g/mol (1.15), 34,000 g/mol (1.15), 124,000 g/mol (1.15), and 801,000 g/mol (1.16). Sodium chloride (NaCl), sodium fluoride (NaF), sodium bromide (NaBr), sodium nitrate (NaNO$_3$), sodium bromate (NaBrO$_3$), sodium chlorate (NaClO$_3$), lithium chloride (LiCl), potassium chloride (KCl), and ammonium chloride (NH$_4$Cl) of analytical grade were purchased from Alpha Chemical Reagents Company. Water for rinsing and preparing all solutions was purified with a Millipore Simplicity 185 purification unit (resistivity $\sim$ 18.2 MΩ cm).

2.2. QCM-D measurements

Experiments were performed with a Q-Sense E1 QCM-D instrument employing a fluid cell hosting a disc-shaped, AT-cut piezoelectric quartz crystal with gold electrodes on each face. These faces were polished to an rms roughness of less than 3 nm, making roughness negligible in data analysis [29]. The fluid cell provided for rapid, non-perturbing exchange of liquid over the operating crystal face. By applying an RF voltage across the electrodes at a frequency near resonance, the crystals were excited to oscillation in the thickness shear mode at their fundamental resonant frequency ($f \approx$ 5 MHz).

Measurements characterizing the changes to crystal resonance behavior due to a surface-adhered film were accomplished by periodically switching on-and-off the driving voltage [27]. When switched off, the voltage decay over the crystal could be fit by an exponentially damped sinusoid, the extracted fitting parameters expressed as the series resonant frequency shift Δf and the dissipation factor ΔD. By switching the driving voltage on and off as rapidly as possible while retaining fittable decays, both parameters were obtained at a time resolution of less than 1 s. With a soft matter film, Δf manifests film mass Δm (including coupled water) and ΔD reflects film frictional (viscous) losses. Provided the film mass is evenly distributed, does not slip at the surface, and is sufficiently rigid and/or thin to have negligible internal friction, the Sauerbrey equation holds,

$$\Delta m = -\frac{\rho_q l_q}{f_o}\frac{\Delta f}{n} = -C\frac{\Delta f}{n} \tag{1}$$

where f_0 is the fundamental frequency, l_q and ρ_q are the thickness and density of the crystal, respectively, C ($=$17.7 ng cm^{-2} Hz^{-1} at f_0) is the mass-sensitivity constant, and $n = 1, 3,\ldots$ is the overtone number [30]. By definition, the dissipation factor can be written

$$\Delta D = E_{\text{dissipated}}/2\pi E_{\text{stored}} \tag{2}$$

where $E_{\text{dissipated}}$ and E_{stored} are, respectively, the energy dissipated and the energy stored during one period of oscillation. The Sauerbrey equation has limited use for visco-elastic polymer films, so film thickness was determined by instrument software that imposes an alternate Voigt model mechanical representation. As done previously in applying this representation [31], densities of PEM and overlying solution were set to 1 g/cm^3, and the solution viscosity was set to 1×10^3 Pa s.

2.3. PEM construction

The gold-coated quartz crystal was cleaned with a 5:1:1 mixture of water, NH$_3$ (25%), and H$_2$O$_2$ (30%) at 75 °C, rinsed with water, and blown dry with a stream of N$_2$. Measurements of PEM growth during LbL deposition started with a change of injection fluid from salt solution (0.5 M NaCl) to PDDA solution (1 mg/mL, 0.5 M NaCl). The latter was exposed to the gold-coated crystal for 25 min before a change of injection to pure water, necessary to ensure a coating of uniform positive charge. After this initial PDDA adsorption, PSS and PDDA solutions were alternatively injected into the cell for 25 min, with intervening 5 min rinses of salt solution (0.5 M NaCl). The final PEM, comprised of eight layer pairs, was designated (PDDA/PSS)$_8$; the capping deposition was of PSS. The two bulk polyelectrolyte samples were used to make all PEMs.

2.4. PEM swelling and PSS uptake

As shown in Fig. 1a, 600 s after assembly of (PDDA/PSS)$_8$, a solution of higher salt concentration was injected into the cell, and after Δf and ΔD had stabilized to within 3 Hz and 1×10^6, respectively, for at least 600 s, a PSS test solution of the same high
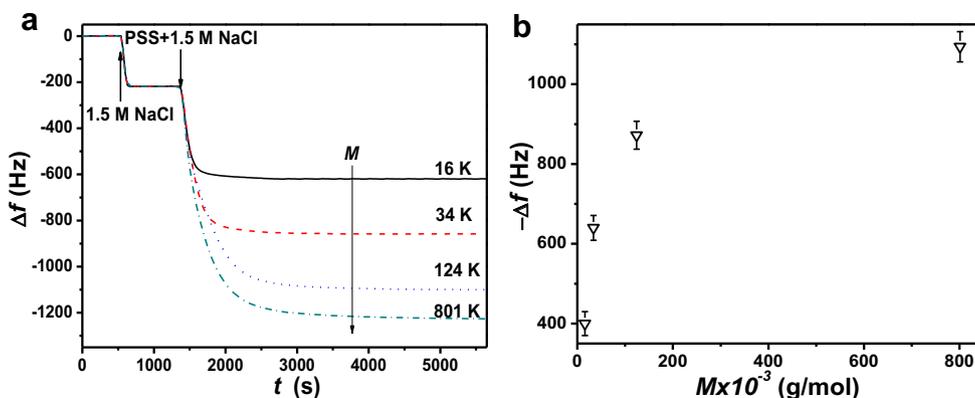
Fig. 1. (a) Frequency shift Δf as a function of time t for the (PDDA/PSS)$_8$ swollen by an initial 0.5 M–1.5 M jump in NaCl concentration at 600 s and subsequent challenge at 1400 s by different M PSS dissolved at the same high NaCl concentration. (b) After the PSS challenges, ultimate $-\Delta f$ shift as a function of M.

salt concentration was injected into the cell. For both exposures, each reported Δf is the average of at least three measurements.

3. Results and discussion

3.1. Mass and thickness changes in the presence of NaCl

Previous studies showed that M has a great influence on PEM assembly [32–36]. A minimum M is required for continuous growth, and failing to meet this minimum, a high M polyelectrolyte will strip the low M oppositely charged polyelectrolyte of the preceding deposition, interrupting the LbL sequence. Further, under continuous growth, M strongly affects the thickness increment of each deposition cycle. To preclude the complicating effects of polydispersity in the current study, the PSS "challengers" were all narrow polydispersity M standards. Fig. 1a displays Δf changes incurred with time t as determined by the current study's test protocol, which was consisted of initial injection of 1.5 M NaCl and subsequent equilibration at this condition, followed by injection of a PSS solution containing 1.5 M NaCl and new equilibration. The downward jump in Δf after the first injection is attributed to the swelling of (PDDA/PSS)$_8$ by salt ions and water, the swelling magnitude correlated with the new salt level. The second downward jump, at injection of PSS, is attributed to PSS uptake by the swollen PEM [28]. Different uptake levels are apparent for different M, the ultimate value of $-\Delta f$ rising with M in the manner displayed in Fig. 1b.

Table 1 lists thickness of PEMs as initially prepared, after swelling by salt, and after uptake of PSS, the highly elevated levels of the latter revealing substantial uptake, especially at high M, where in some cases, thickness doubled. Thicknesses are computed under the reasonable approximation that all PEMs have the same uniform density, chosen as 1.0 g/cm^3, making thickness change proportional to mass uptake. Because of approximations in obtaining mass and thickness from QCM-D measurements, mass

and thickness are both regarded as semiquantitative. Trends of uptake with M are inconsistent with the simple exchange of low M PSS for high M PSS inasmuch as substantial uptake (up to 50% increase) occurs even when the PSS challenger has lower M than the PSS employed in PEM construction.

PEM swelling at an elevated salt level is necessary for subsequent uptake of PSS; at elevated salt, the greater presence of small ions within the PEM exposes fixed ion exchange sites amenable to PSS exchange [28]. After such a large jump in salt concentration, from 0.5 M – the level at PEM construction – to 1.5 M, from where PDDA/PSS LbL build-up is linear to where LbL build-up is exponential, the PEM is primed for permeation of PSS across the entire PEM thickness, at least for most of the M range examined. Indeed, the physical underpinnings of exponential LbL growth appear similar to those of uptake. If each positive site created by salt infusion exchanges with just one PSS chain, the mass of PSS added to the PEM would be linear in M. The same linearity would likely apply even in light of ancillary changes to PEM water content. Fig. 1b indicates, instead, that the M dependence weakens and saturates with M, arguing that PSS chains, at least at high enough M, exchange with multiple PEM sites in proportion to M. Several arguments can plausibly explain M saturation. In one, uptake is kinetically limited at high M, with the period of observation too short for full PSS penetration. Since this possibility seems incompatible with the time course of uptake plotted in Fig. 1a, we instead favor arguments postulating that steady state uptake is thermodynamically limited. Here, as PSS content rises, the unfavorable segmental interaction between the two polyelectrolytes could create a PSS solubility limit. Or, the immobility of the PEM's PDDA component could frame spatial constraints, in essence a fixed network, that impose an M-dependent confinement entropy on the incoming PSS. Our experiments cannot distinguish between the two thermodynamic arguments. In the previous study of PSS uptake by salt-swollen PEMs, only polydisperse PSS-0 was examined: its uptake closely approximates the uptake seen here for PSS-3, which nominally has a much higher M. This apparent inconsistency highlights the need for uptake studies with nearly monodisperse polyelectrolyte samples.

As PEMs incorporate increasing levels of small ions and water, ΔD grows, reflecting the 'loosening' of PEM structure with swelling. Ultimate values of ΔD after uptake by PSS are plotted against M in Fig. 2a; the figure reveals that water and/or small ion uptake(s) accompany PSS uptake, more so at higher M. Origins of the ΔD rise are not entirely clear and neither are the actual levels of water and/or ions trapped within the PEM. Nonetheless, the trend establishes

Table 1
PEM thickness as assembled, after swelling by NaCl and after PSS uptake (units: nm).

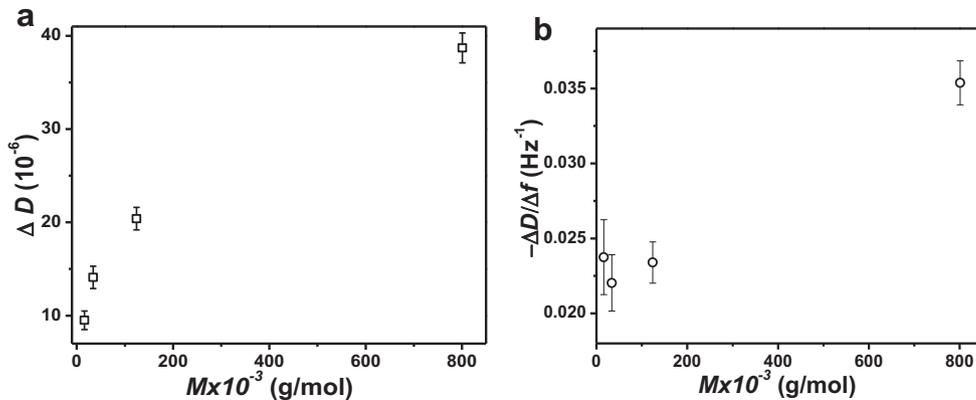| PSS challenger	As assembled	1.5 M NaCl		0.75 M NaCl	
		After salt swelling	After PSS uptake	After salt swelling	After PSS uptake
PSS-1	180	214	303	185	244
PSS-2			353		268
PSS-3			408		286
PSS-4			437		288

Fig. 2. M dependence of ultimate values for (a) ΔD and (b) $\Delta D/(-\Delta f)$. Both at 1.5 M NaCl.

that the PEM-captured PSS continues to bear a substantial fraction of small counterions along with their waters of hydration, an unsurprising effect given that, at such high salt concentration, polyelectrolyte charges in the PEM are mostly compensated with small ions. It has been reported that the ratio $\Delta D/(-\Delta f)$ gives insight into the structure/dynamics of adsorbed protein layers [37]. Fig. 2b plots this ratio against M for ultimate PSS uptake, and on this plot, PSS-4 appears to be an outlier, its sharply higher value arguing that the surface of the modified PEM is different from that of the other, lower M samples. This different surface might reflect incomplete PEM penetration or possibly the presence of larger, looser loops and tails.

To understand better how M affects PSS penetration, Δf and ΔD were recorded for PSS challenges at 0.75 M NaCl, a lower salt concentration corresponding to a tighter, less swollen PEM. A previous study at this concentration established that PSS-0, of moderate M and broad polydispersity, was mostly trapped on/near the PEM surface [28]. Fig. 3 shows that Δf increases with M in a manner reminiscent of the experiment at 1.5 M NaCl. However, Δf levels off at lower M, consistent with a smaller M exclusion limit for a tighter PEM structure. Once again, $\Delta D/(-\Delta f)$ is anomalously high for M at saturation (data not shown), as expected for the trapping of PSS on/near the PEM surface. The PEM thicknesses corresponding to all these trends are given in Table 1.
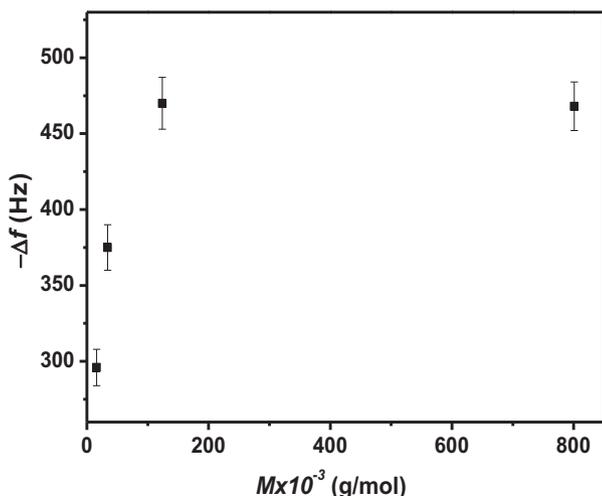
3.2. PSS uptake kinetics in the presence of NaCl

In a previous report, PSS-0 uptake was examined as a function of NaCl concentration, and a higher concentration, substantially above that maintained during PEM construction, led to more and faster PSS uptake. Surprisingly, the uptake kinetics for this sample at high NaCl concentration (>1 M NaCl for PEMs prepared at 0.5 M NaCl) were accurately fit by an equation derived on assumption that uptake is controlled by PSS diffusion in the PEM; this finding strongly argues that highly salt-swollen PEMs are uniformly permeable in their depth to polyelectrolyte diffusion. At lower salt concentrations, closer to that of PEM construction (0.75 M NaCl for PEMs made at 0.5 M NaCl), the same experiments suggested that PSS might be trapped on/near the PEM surface, unable to penetrate the film fully. These conclusions, unfortunately, were somewhat confounded by the large polydispersity of PSS-0.

The uptake kinetics recorded here for nearly monodisperse PSS samples are consistent with our previous findings for polydisperse PSS [28]. At high polymer concentration, the traces of Fig. 4, plotting uptake after abrupt challenges of PSS-3 dissolved in 1.5 M NaCl, are consistent with predictions for the diffusive penetration of the entire film, with ultimate uptake achieved only after 20 min or longer. Fitting the initial linear transients of plots of mass uptake against $t^{1/2}$, diffusion coefficients D of $(8.2 \pm 1) \times 10^{-13}$ and
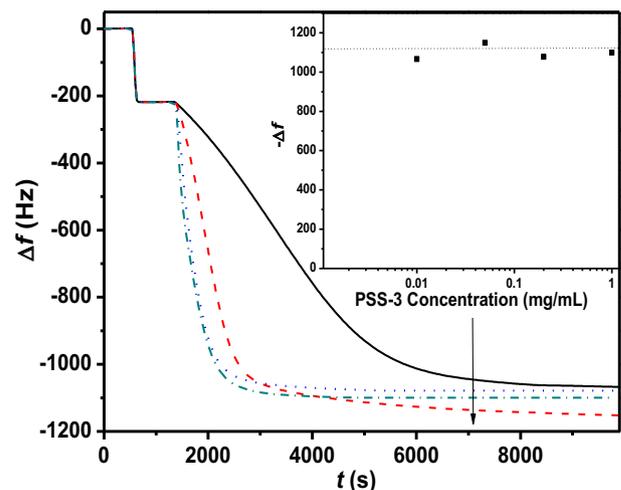

Fig. 3. Dependence of Δf on M at 0.75 M NaCl. Saturation is noted for M above 150,000 g/mol.

Fig. 4. Δf plotted against t at 1.5 M NaCl for the swelling and subsequent uptake of PSS-3 by (PDDA/PSS)$_8$ for polymer concentrations of 0.01, 0.05, 0.2 and 1.0 mg/mL. The inset demonstrates the concentration-independence of ultimate uptake.

$(9.5 \pm 1) \times 10^{-13}$ cm^2/s are calculated for PSS-3 solution concentrations of 0.2 and 1.0 mg/mL, respectively. As the two D values are equal to within experimental error, uptake control by diffusive transport in PEM is verified. At lower PSS concentrations, similarly extracted D values are somewhat lower and mass uptake does not coincide with the predicted transient diffusion form, discrepancies traceable to a shift from PSS transport dominated by diffusion in PEM to PSS transport dominated by diffusion in solution. Fig. 4, which plots uptake against t for several polymer concentrations in the range of 0.01–1.0 mg/mL, makes the transport shift evident, the solution-controlled diffusion regime, starting (with decreasing polymer concentration) at ~0.01 mg/mL, characterized by much slower uptake. This crossover concentration is qualitatively consistent with predictions of a simple model for transient serial diffusion through solution and film. Our previous publication detailed how D values are obtained from raw QCM-D data. Because the PEM mass changes significantly during uptake (sometimes doubling), there is a minor inaccuracy in applying the standard transient diffusion model, which considers that PEM mass, and thus PEM thickness, are constant; with this modeling inaccuracy, extracted D values by our method should be viewed as "apparent". The inset to Fig. 4 indicates that, aside from negligible impact on D, polymer concentration in this dilute regime negligibly impacts ultimate uptake.

Adopting a standard PSS concentration of 1 mg/mL, D in the PEM for narrow distribution PSS-1, PSS-2, PSS-3, and PSS-4 were obtained at 1.5 M NaCl by the same uptake procedure, and these values are given in Table 2. Mass uptake conforms to uniform penetration of PEM under PSS diffusion control. In our previous study, only the broadly distributed PSS-0 was examined, and its polydispersity obscured interpretation. Not too surprisingly, when full permeation is possible, D falls with M, although the data are too limited to infer the precise M dependence of the fall. As noted in the previous publication, absolute values of D are remarkably high, showing that high NaCl has effectively "plasticized" the PEM.

3.3. PEM swelling and PSS uptake in the presence of different anions

For anions, the conformational stability of proteins in aqueous solution follows the classic Hofmeister series: $ClO_4^- > SCN^- > I^- > NO_3^- > Br^- > Cl^- > CH_3COO^- > HCOO^- > F^- > OH^- > HPO_4^{2-} > SO_4^{2-}$. (Depending on the property measured, the order may vary.) Ions to the right of Cl^- in the series are known as kosmotropes, which interact strongly with water and are highly hydrated (more hydrophilic), while ions to the left are known as chaotropes, which interact weakly with water and are less hydrated (more hydrophobic). Although these (and other) physical interpretations of the Hofmeister series are debated [38,39], the debate's implications for the current experimental study are few. With $(PDDA/PSS)_n$ PEMs, layer thickness was reported in literature to track closely with counteranion position in the Hofmeister series, a correlation presumably manifesting the relative strength of counterion-to-polycation binding [25,40]; less hydrated counterions, with smaller negative hydration entropies and smaller hydrated sizes, bind more strongly to polycations, argued to

produce a more loopy surface conformation. In a second, concurring study, PEMs of different composition were reported to grow more rapidly in the presence of loosely bound I^- than tightly bound F^-, although a different physical picture was advanced [41]. Other literature reports that counterion identities affect the mechanical and swelling properties of PEMs [42–44]. From these precedents, anion identity can be expected to alter both PEM swelling at elevated salt levels as well as PSS uptake after such swelling.

For a variety of sodium salt anions, all at 0.75 M, Fig. 5 plots Δf against t during the initial swelling and the subsequent uptake of PSS-3 into $(PDDA/PSS)_8$. At both challenges, the anion identity dramatically affected the levels of swelling and uptake. Fig. 6a shows that for the initial swelling step, ultimate values of Δf follow $Br^- > NO_3^- > ClO_3^- > Cl^- > BrO_3^- > F^-$, an order approximately opposite to that for absolute values of ion hydration entropy. As noted before, less hydrated anions bind more strongly to polycations [40,45], suggesting that the larger swelling is a consequence of the weakening of polyion–polyion contacts, the ion exchange equilibrium thereby effectively shifted toward polyion-counterion contacts. (The recently proposed law of matching water affinities provides a slightly different, equally satisfactory physical explanation for the observed ordering of swelling for different ions [46].) Several investigators report that PEMs swell less when exposed to poorly hydrated anions [42–44], the opposite trend. The counterion concentrations of these investigations were extremely low, so ion infusion did little to weaken polyion–polyion contacts. Water content was nevertheless slightly lowered during infusion, since weakly hydrated counteranions convey to PEM less water than counterions that are strongly hydrated. The two effects compete, the first dominating at larger salt concentrations and the second at lower salt concentrations.

Focusing again on Fig. 5, PSS challenges are seen to produce Δf changes comparable to, and even larger than, those incurred by PEM swelling at elevated salt levels, although the underlying mass growth is slower. For the different counteranions, Fig. 6b presents limiting PSS uptake Δf values at $t = 8000$ s; not all uptake curves have saturated, so the limiting values are not all ultimate uptakes. In our previous report for PSS-0 uptake after a jump from 0.5 M NaCl (level at PEM construction) to 0.75 M NaCl, the polyanion was judged to be mostly trapped on/near the PEM surface, but at 1.5 M and higher, with the PEM much more swollen, the same polyion sample penetrated and diffused throughout the PEM. Uptake kinetics inconsistent with diffusive permeation are a key characteristic of trapping. Searching for this characteristic in the curves of
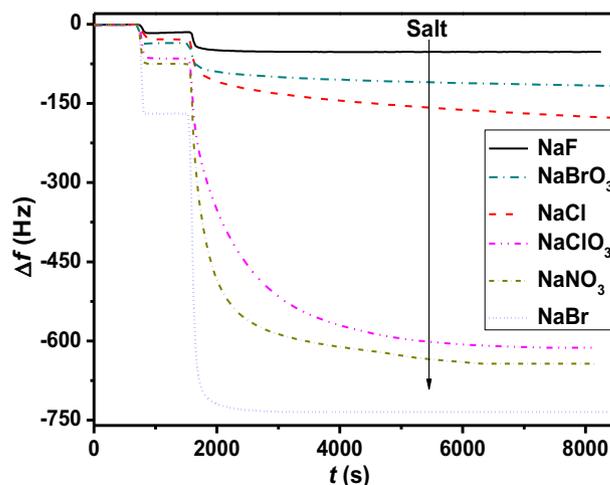
Table 2
PSS diffusion coefficients D in PEMs swollen by 1.5 M NaCl.

sample	D ($\times 10^{-13}$ cm^2/s)
PSS-1	43
PSS-2	19
PSS-3	9.5
PSS-4	9.5

Fig. 5. Δf vs. t for the swelling and subsequent uptake of PSS-3 by $(PDDA/PSS)_8$ in the presence of various 0.75 M salts.
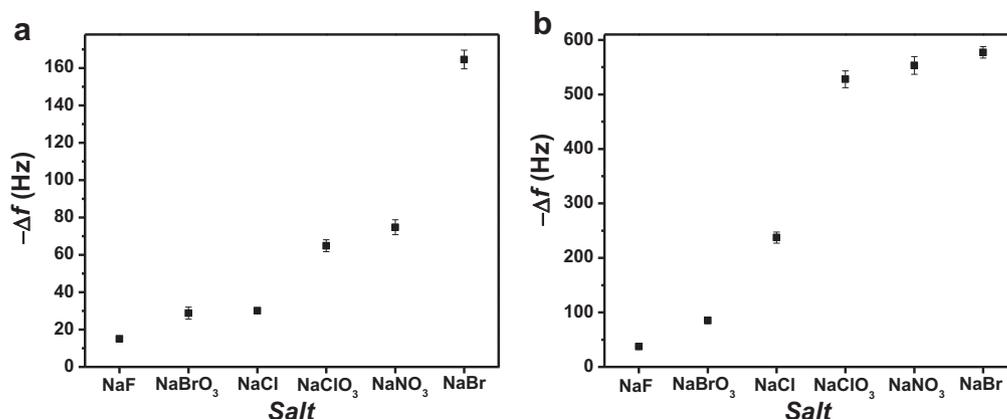
Fig. 6. For different salt anions, the limiting values of Δf after (a) swelling of PEM upon jump from 0.5 to 0.75 M salt and (b) PSS-3 uptake.

Fig. 5, diffusive PSS uptake is deduced for counterions less hydrated than Cl^-, while trapping is deduced for those that are more hydrated. Another characteristic of diffusive penetration is rapidly saturated PSS uptake, a trend clearly reflected in Fig. 6b for the salts with less hydrated anions plotted to the right of NaCl. The figure's form is consistent with a reasonably sharp transition from trapping to diffusive permeation at intermediate swelling, the transition encountered equally by varying salt concentration or anion identity.

4. Conclusions

Swelling by a jump in salt concentration allows a polyanion-capped PEM to gain substantial additional amounts of polyanion from a bathing solution. Here, polyanion uptake was demonstrated through QCM-D experiments on a PEM system incorporating a monodisperse polyanion, with control over the uptake exerted through polyanion molecular weight and degree of PEM swelling. For the latter, above a threshold swelling, capture and diffusion allows full permeation of the PEM by the added polyanion, with saturated polyion uptake obtained over short, diffusion-limited transport times. Below the threshold, polyanion uptake is lower, the polyanion remaining trapped near the PEM surface, much as the case for polyanions during ordinary LbL deposition. Swelling is principally a function of the degree to which salt ions compete for ion exchange sites of the two polyelectrolytes, and so the salt ion identity and the size of the jump in salt concentration are both important to uptake. Differences in affinities of the salt ions for the polyelectrolytes track, as expected, with positions of these ions in the Hofmeister series. Significant issues remain unresolved. One is the M-dependence of uptake in the regime where added polyanion fully penetrates the PEM (see Fig. 3), and another is retention (or not) of the PEM's layered structure when swollen by salt or confounded by polyanion uptake. There is, as yet, no model that predicts the level of polyion uptake or the values of D that determine the kinetics of this uptake for swollen PEMs. Lastly, factors that determine the swelling threshold for full PEM permeation by polyanion challenger are not quantitatively understood. Despite the open questions, the current results give valuable conceptual insights into PEM assembly and provide important guidance to development of new approaches for PEM modification.

Appendix A. Supplementary meterial

Supplementary data related to this article can be found at http://dx.doi.org/10.1016/j.polymer.2012.09.011.

References

[1] Shirazi M, van de Ven TGM, Garnier G. Langmuir 2003;19:10829.
[2] Bysell H, Malmsten M. Langmuir 2006;22:5476.
[3] Kabanov VA, Skobeleva VB, Rogacheva VB, Zezin AB. J Phys Chem B 1485; 2004:108.
[4] Horvath AT, Horvath AE, Lindström T, Wågberg L. Langmuir 2008;24:6585.
[5] Horvath AT, Horvath AE, Lindström T, Wågberg L. Langmuir 2008;24:7857.
[6] Horvath AT, Horvath AE, Lindström T, Wågberg L. Langmuir 2008;24:10797.
[7] Wågberg L, Hägglund R. Langmuir 2001;17:1096.
[8] Takemoto Y, Ajiro H, Asoh T, Akashi M. Chem Mater 2010;22:2923.
[9] Stuart MAC, Fleer GJ, Lyklema J, Norde W, Scheutjens JMHM. Adv Colloid Interfac 1991;34:477.
[10] Ikeda S, Tsunoda MA, Maeda H. J Colloid Interfac Sci 1979;70:448.
[11] Vandesteeg HGM, Stuart MAC, Dekeizer A, Bijsterbosch BH. Langmuir 1992;8: 2538.
[12] Dobrynin AV, Deshkovski A, Rubinstein M. Macromolecules 2001;34:3421.
[13] Netz RR, Joanny JF. Macromolecules 1999;32:9013.
[14] Park JM, Muhoberac BB, Dubin PL, Xia JL. Macromolecules 1992;25:290.
[15] Chen HL, Morawetz H. Macromolecules 1982;15:1445.
[16] Bakeev KN, Izumrudov VA, Kuchanov SI, Zezin AB, Kabanov VA. Macromolecules 1992;25:4249.
[17] Skepö M, Linse P. Macromolecules 2003;36:508.
[18] Carlsson F, Linse P, Malmsten M. J Phys Chem B 2001;105:9040.
[19] Carlsson F, Malmsten M, Linse P. J Am Chem Soc 2003;125:3140.
[20] Bysell H, Malmsten M. Langmuir 2009;25:522.
[21] Dautzenberg H. Macromolecules 1997;30:7810.
[22] Jomaa HW, Schlenoff JB. Macromolecules 2005;38:8473.
[23] Decher G. Science 1997;277:1232.
[24] Nazaran P, Bosio V, Jaeger W, Anghel DF, von Klitzing R. J Phys Chem B 2007; 111:8572.
[25] Dubas ST, Schlenoff JB. Macromolecules 1999;32:8153.
[26] McAloney RA, Sinyor M, Dudnik V, Goh MC. Langmuir 2001;17:6655.
[27] Rodahl M, Höök F, Krozer A, Brzezinski P, Kasemo B. Rev Sci Instru 1995;66: 3924.
[28] Zan XJ, Peng B, Hoagland DA, Su ZH. Polym Chem 2011;2:2581.
[29] Martin SJ, Frye GC, Ricco AJ, Senturia SD. Anal Chem 1993;65:2910.
[30] Serizawa T, Yamamoto K, Akashi M. Langmuir 1999;15:4682.
[31] Liu GM, Zou SR, Fu L, Zhang GZ. J Phys Chem B 2008;112:4167.
[32] Porcel C, Lavalle P, Decher G, Senger B, Voegel JC, Schaaf P. Langmuir 2007;23: 1898.
[33] Sui ZJ, Salloum D, Schlenoff JB. Langmuir 2003;19:2491.
[34] Sun B, Jewell CM, Fredin NJ, Lynn DM. Langmuir 2007;23:8452.
[35] Richert L, Lavalle P, Payan E, Shu XZ, Prestwich GD, Stoltz JF, et al. Langmuir 2004;20:448.
[36] Kujawa P, Moraille P, Sanchez J, Badia A, Winnik FM. J Am Chem Soc 2005; 127:9224.

[37] Hemmersam AG, Foss M, Chevallier J, Besenbacher F. Colloid Surface B 2005; 43:208.
[38] Zhang YJ, Cremer PS. Annu Rev Phys Chem 2010;61:63.
[39] Marcus Y. Chem Rev 2009;109:1346.
[40] Salomäki M, Tervasmäki P, Areva S, Kankare J. Langmuir 2004;20:3679.
[41] Mermut O, Barrett CJ. J Phys Chem B 2003;107:2525.
[42] El Haitami AE, Martel D, Ball V, Nguyen HC, Gonthier E, Labbé P, et al. Langmuir 2009;25:2282.
[43] Salomäki M, Laiho T, Kankare J. Macromolecules 2004;37:9585.
[44] Salomäki M, Kankare J. Macromolecules 2008;41:4423.
[45] Schlenoff JB, Rmaile AH, Bucur CB. J Am Chem Soc 2008;130:13589.
[46] Collins KD, Neilson GW, Enderby JE. Biophys Chem 2007;128:95.